Escola de Primavera de Transição e Turbulência Blumenau 2022
ABCM
13th Spring School on Transition and Turbulence
September 19th-23rd, 2022, Blumenau, SC, Brazil

EPTT-2022-0071
DNS of Gas-Liquid Stratified Flow Using Second-Order Finite Volume Method

Victor W. F. de Azevedo
Department of Engineering and Technology, Federal Rural University of the Semi-arid Region, 59625-900, Mossoró-RN, Brazil
victorwfreire@ufersa.edu.br
Emilio E. Paladino
SINMEC Lab, Department of Mechanical Engineering, Federal University of Santa Catarina, 88040-900, Florianópolis-SC, Brazil
emilio.paladino@ufsc.br

Abstract. *Stratified flows are encountered in many forms in industrial processes and in nature. Through many years the spectral methods were applied to study turbulence however these methods are not easily applied to complex flow situations such as multiphase flows. Such methods were mostly applied in fluid-bounded domains when solving stratified flows, which is focused on the near-interface turbulence and not in the bulk flow wall-bounded behaviour. Wall-bounded domains were solved in the last years based on RANS models, nonetheless, the present work performed DNS based on the Second-Order Finite Volume Method discretization to solve stratified gas-liquid flow. The interface was captured with CICSAM and the interface curvature calculated based on the Height-Functions method. The results confirmed the already consolidated resemblance between gas-phase and wall turbulence statistics. The present model showed that DNS for stratified flow is possible based on low-order discretization of governing equations.*

Keywords: *Direct Numerical Simulation, stratified flow, near-interface turbulence*

1. INTRODUCTION

Multiphase flows are present in many applications, the analysis of such flows also with turbulence modelling has been theme of study in the past years. These kinds of studies combine the well-known complexity of turbulence with the presence of interfaces, which can affect flow structure. Even though most of the models developed in the past applied spectral methods to discretize the governing equations, the application of finite-difference-based methods in Direct Numerical Simulations (DNS) is still valid.

DNS studies of multiphase flows found their basis on single-phase channel flow studies with the classic DNS performed in the channel flow by Kim *et al.* (1987). Their consolidated methodology inspired the first studies of near-interface turbulence by Lombardi *et al.* (1996) and de Angelis *et al.* (1997), whose works performed DNS in a gas-liquid stratified flow considering plain and wavy non-deformable interfaces, respectively; nonetheless, a fractal time-step was applied for the transient term. Both works showed that near-interface turbulence structure resembles near-wall's in the gas phase. The study of deformable interfaces began with Fulgosi *et al.* (2003), whose work followed the same referred pseudoespectral method as the previous cited works, however, considered the interface displacement given by an advection equation for the volume fraction. The flow was also studied at the gas side and the results showed that a certain damping is present in turbulence in the near-interface region against the near-wall region. The obtained results allowed the proposition of a damping function (Lakehal *et al.*, 2005) which was later on applied in a large-eddy simulation (LES) in the work of Liovic and Lakehal (2007), whose results approximately matched the DNS results for the stratified flow. Alternatively, in wall-bounded flows, the Egorov approach can be used to model near-interface turbulence, which imposes a wall-like treatment to the near-interface region (Egorov *et al.*, 2004). The work of Frederix *et al.* (2018) tested different turbulence models in a co-current stratified flow and obtained good results compared to experimental data taking into account the near-interface turbulence damping. This model, was improved later by Fan and Anglart (2019) to allow the aplicaton of it to the volume-of-fluid (VOF) method, independent of the interface reconstruction method adopted.

The application of finite-difference-based methods in DNS is still theme of debate. Based on our research only the work of Eggels *et al.* (1993) applied the finite volume method (FVM) in DNS of horizontal stratified flow. Recent works are applying Reynolds-averaged Navier-Stokes (RANS) models to solve the flow (Tekavčič *et al.*, 2021) and obtaining good results against experimental data, however, such models apply means in the solution of governing equations which could "hide" flow details. This leaves margin for the development of DNS based on FVM in more complex flows situations as multiphase flows, which is not always possible through the application of spectral methods.

The present study performed DNS in a stratified channel flow using second-order FVM to discretize the equations and solving the flow in physical (not spectral) space. The domain is wall-bounded against the fluid-bounded of the previous cited works (Lombardi *et al.*, 1996; de Angelis *et al.*, 1997; Fulgosi *et al.*, 2003), which makes possible the analysis of the possible influence of the wall boundary at the interface. The methology was validated based on DNS of single-phase channel flow (de Azevedo *et al.*, 2021).

2. COMPUTATIONAL MODEL

2.1 Governing equations

The problem is governed by momentum equations for incompressible flow

$$\frac{\partial \rho u_i}{\partial t} + \frac{\partial (\rho u_j u_i)}{\partial x_j} = -\frac{\partial p}{\partial x_i} + \frac{\partial}{\partial x_j}\left[\mu\left(\frac{\partial u_i}{\partial x_j} + \frac{\partial u_j}{\partial x_i}\right)\right] + \rho g \tag{1}$$

where u_i denote fluid velocity components, p the pressure, t denotes physical time, ρ denotes fluid density and μ denotes fluid viscosity, which are defined respectively as

$$\rho = \alpha\rho_L + (1-\alpha)\rho_G \tag{2}$$

and

$$\mu = \alpha\mu_L + (1-\alpha)\mu_G \tag{3}$$

in the VOF method, where α denotes the volume fraction. The volume fraction is advected following the CICSAM scheme (Ubbink and Issa, 1999) and the problem is also governed by the continuity equation

$$\frac{\partial \rho u_i}{\partial x_i} = 0. \tag{4}$$

2.2 Model set-up

DNS in a gas-liquid stratified channel flow with Reynolds number based on the friction velocity of $Re_\tau \approx 180$ is performed with a second-order finite-volume framework, which solves mass and momentum equations in a VOF-framework considering a coupled solution and a pressure-based solver (Denner and van Wachem, 2014). The normal boundaries (y-direction) were set as no-slip walls, while the stream-wise (x-direction) and span-wise (z-direction) boundaries were set as periodic. Along with the already mentioned advection of volume fraction scheme, the interface curvature is calculated using the height-functions (HF) method.

The flow was initialized with a parabolic velocity profile and it was driven by momentum source in the stream-wise direction, which considers constant pressure gradient – necessary owing to the periodic boundary condition in the stream-wise direction. This source was set in a way that balances the momentum dissipation by the wall shear stress as

$$\frac{\Delta p}{\Delta x} = \frac{Re_{\tau_L}\nu_L^2\rho_L}{\delta^3} = \frac{Re_{\tau_G}\nu_G^2\rho_G}{\delta^3}, \tag{5}$$

where δ is the integral length scale, ρ the density and ν the cinematic viscosity of the respective liquid (L) or gas (G) phase. In this way, the wall shear stress is based on the Reynolds number

$$Re_\tau = \frac{u_\tau \delta}{\nu}, \tag{6}$$

which, based on the interface coupling condition: $\tau_{I_G} = \tau_{I_L}$, it can be found that

$$Re_{\tau_G} = \frac{\sqrt{\rho_L}}{\sqrt{\rho_G}}\frac{\nu_L}{\nu_G} Re_{\tau_L}. \tag{7}$$

Therefore, the source term for each phase will only depend on the prescribed Reynolds number based on friction velocity, fluid properties and channel size. The fluid properties of gas and liquid are determined in a way that Eq. 7 gives $Re_{\tau_L} \approx Re_{\tau_G} \approx 180$.

The computational box has dimensions $4\pi\delta$ x 4δ x $2\pi\delta$ in the stream-wise, normal and span-wise directions, respectively. For the present case, the computational mesh needs to be refined near the walls and both sides of interface, in order to capture turbulence phenomena on these regions. Hence, the mesh was refined following the relation

$$y(\xi) = \begin{cases} \frac{\delta_f}{2}\left[1 - \frac{tanh\{\beta(1-2\xi_L)\}}{tanh(\beta)}\right], & \text{if liquid side} \\ \frac{\delta_f}{2}\left[1 - \frac{tanh\{\beta(1-2\xi_G)\}}{tanh(\beta)}\right] + \delta_f, & \text{otherwise,} \end{cases} \tag{8}$$

where $\xi_L = y/\delta_f$,

$$\xi_G = \frac{y-\delta_f}{L-\delta_f},$$

δ_f denotes the interface position ($\delta_f = 2\delta$ in the present work) and L the total normal length of the merged domain. Following Eq. 8, it was reached a $\Delta y^+ \approx 0.8$ near the walls and both sides of the interface, based on the applied clustering factor β and the obtained velocity scales at both phases, where

$$\Delta y_i^+ = \frac{u_{\tau_i} \Delta y_i}{\nu_i}. \tag{9}$$

Hence, we assure that the first volume away from the wall and interface is within the viscous sub-layer.

In the present work, the flow was initialised with the generation of a von-Karman spectrum, which estimates the velocity fluctuations based on an initial turbulent kinetic energy and length scale δ, considering isotropic homogeneous turbulence. The obtained velocity fluctuations are added to an initial parabolic velocity field profile, thus constituting the "perturbed" initial velocity field. This methodology worked well for single-phase channel flow (de Azevedo *et al.*, 2021), however, when applied to the stratified flow domain lead to a chaotic velocity field which resulted in interface breakup. The solution for this issue was to initialise the gas and liquid phases separately as two "single-phase flows" and allow the velocity fields to develop. Once the fields were determined to be in the statistically developed regime, the single-phase flow velocity field for each phase was saved and merged to form one single computational domain – the stratified flow domain (see Fig. 1).

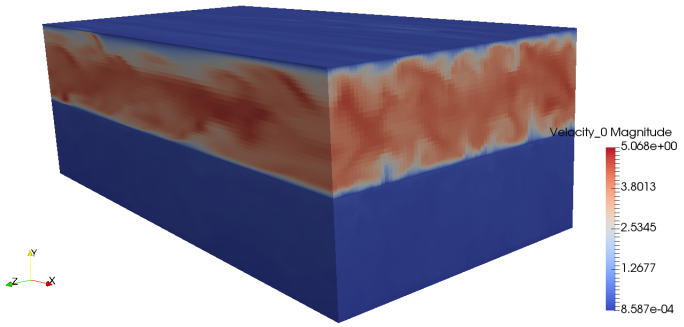

Figure 1: Initial velocity field for the stratified flow. The gas phase on top and the liquid phase in the bottom half. The colors indicate the velocity magnitude of each phase.

Additional to model set-up, the capillary time-step (Denner and van Wachem, 2015) is applied to maintain the interface sharp and a surface tension coefficient based on the $\sqrt{Fr}/We$ relation (considering the capillary waves regime, as applied in Zonta *et al.* (2016)) is also applied in the present work.

Based on our studies, taking into account DNS in a single-phase channel flow, a computational mesh of 512 x 256 x 128 cells in the stream-wise, normal and span-wise direction, respectively, as presented in Tab. 1 was applied to the present study.

Case Id	**Box size**	N_x x N_y x N_z	Δx^+	Δy_c^+	Δz^+
Mesh 2 Gas	$4\pi\delta$ x 2δ x $2\pi\delta$	512 x 128 x 128	5.13	4.70	2.56
Mesh 2 Liquid	$4\pi\delta$ x 2δ x $2\pi\delta$	512 x 128 x 128	4.54	4.15	2.27

Table 1: Computational meshes applied in initialization process. These meshes are merged in order to constitute the stratified flow domain. Δy_c^+ represents the values of Δy in the center portion of the domain.

3. RESULTS

This section presents the results obtained based on the described methodology. The results were compared to the single-phase channel flow results obtained in de Azevedo *et al.* (2021) following the same methodology.

3.1 Velocity fluctuations

Velocity fluctuations are obtained based on the Reynolds decomposition

$$u_i = \langle u_i \rangle + u_i', \tag{10}$$

where the means $\langle\rangle$ are performed in stream- and span-wise directions and also in time; u_i is the instant velocity and u_i' the velocity fluctuations.

Results for the stratified flow, considering the near-interface reference in the gas phase, are presented in Fig. 2 and compared to results for the single-phase channel flow (denoted by the dots). The colors refers to the different components of velocity fluctuations: black for stream-wise, red for normal and blue for span-wise.

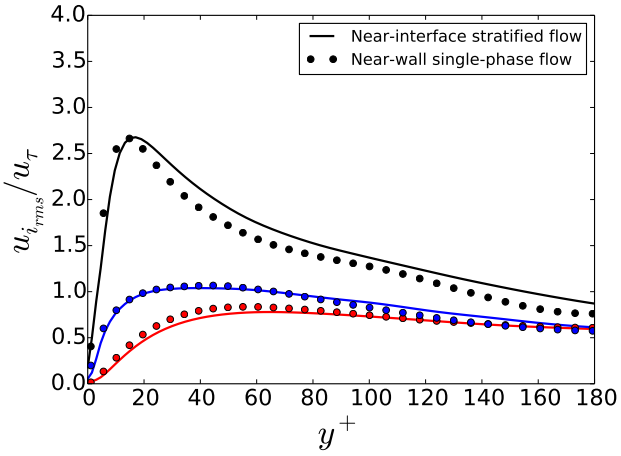

Figure 2: Velocity fluctuations. The continuous lines represent near-interface values for the stratified flow, the dots are the DNS results for single-phase flow.

The behaviour of the velocity fluctuations in the stratified flow resembles the near-wall behaviour in single-phase flow, as already commented in literature (Fulgosi *et al.*, 2003).

3.2 Autocorrelations

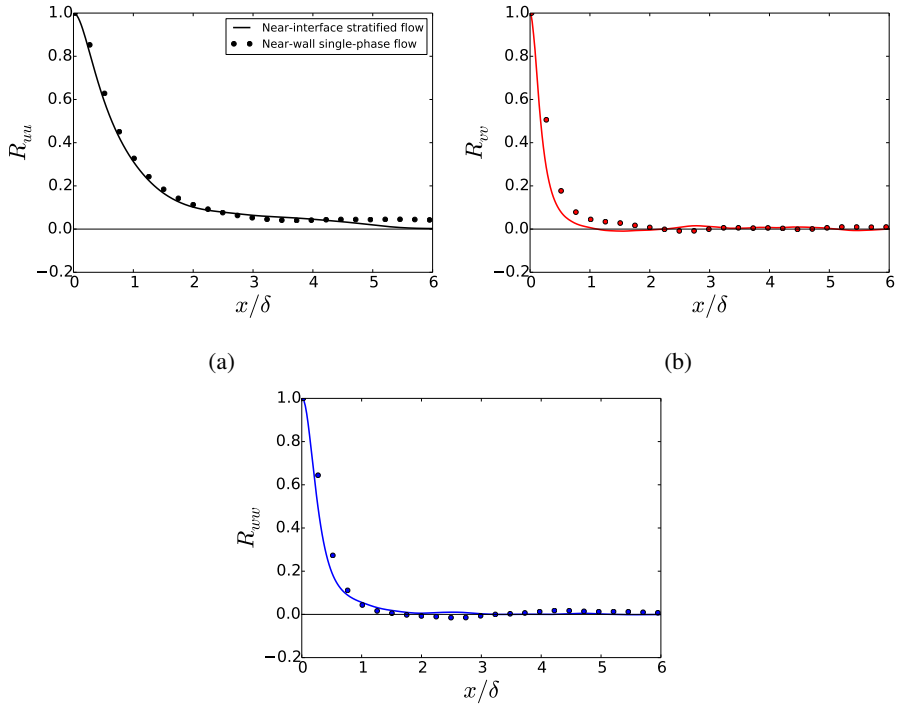

Figure 3: Autocorrelation functions in the stream-wise direction in the near-interface compared to the near-wall region for the single-phase flow: (a) Autocorrelation of u-fluctuations, (b) Autocorrelation of v-fluctuations and (c) Autocorrelation of w-fluctuations. The continuous lines represents the near-interface region and the dots the near-wall region for the single-phase flow.

The similarity between near-interface and -wall behaviour can also be analysed through the autocorrelation functions. Once turbulence affects the entire domain, one can not describe the flow behaviour through "local" informations rather than variables that take into account the entire flow, as two-point correlations (Silveira Neto, 2020).

The autocorrelation functions of the velocity fluctuations can be obtained by (Pope, 2001)

$$R_{ii}(\mathbf{r},t) = \frac{\langle u_i'(\mathbf{x}+\mathbf{r},t)u_i'(\mathbf{x},t)\rangle}{\langle u_i'u_i'\rangle}. \tag{11}$$

Results for the near-interface autocorrelation functions at $y^+ \approx 5$ are compared to near-wall values obtained for the single-phase flow in Fig. 3 in the stream-wise direction. The results for the near-interface region remained close to near-wall region in the single-phase flow, which confirms the statement of the previous section of the present work of the similarity between near-wall and -interface turbulence statistics.

Even though the capillary waves regime did not influenced the stream-wise autocorrelation functions, some differences between near-interface and -wall results are shown in Fig. 4 for the stratified flow and compared to single-phase flow. According to Kim *et al.* (1987), the separation between the down peak in the span-wise autocorrelation function is a good estimation of the mean spacing between streaks (equivalent to twice this distance). Looking at Fig. 4b, one can note slightly difference between the down peaks of the stratified and single-phase flows, while Fig. 4c shows a very close behaviour between near-interface and near-wall regions. In Fig. 4a, the down peak for the near-interface region did not reach the negative values of the single-phase flow. These differences shows a certain influence of the capillary waves regime in turbulence statistics in the near-interface region against near-wall region.

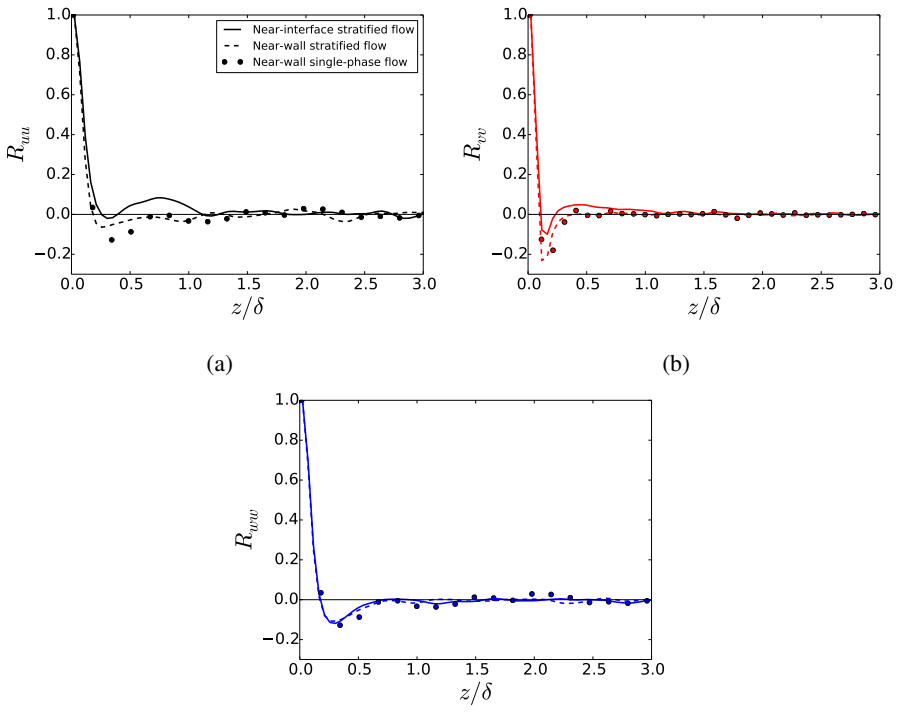

Figure 4: Autocorrelation functions in the span-wise direction evaluated near the wall region in single-phase flow and near the interface in stratified flow: (a) Autocorrelation of u-fluctuations, (b) Autocorrelation of v-fluctuations and (c) Autocorrelation of w-fluctuations. The continuous lines represents the near-interface region, the dashed lines the near-wall region for the stratified flow and the dots the near-wall region for the single-phase flow.

3.3 Turbulent Kinetic Energy budget

The turbulent kinetic energy (TKE) budget is given by (Tennekes *et al.*, 1972)

$$\frac{\partial k}{\partial t} + \frac{\partial (u_i k)}{\partial x_i} = \underbrace{-\left\langle u_i' u_j' \right\rangle \frac{\partial u_i}{\partial x_j}}_{\text{Production}} \underbrace{- \frac{1}{\rho}\frac{\partial}{\partial x_i}\left\langle p u_i' \right\rangle}_{\text{Press. Diffusion}} \underbrace{- \frac{1}{2}\frac{\partial}{\partial x_j}\left\langle u_i' u_i' u_j' \right\rangle}_{\text{Turb. Transport}} + \underbrace{\frac{1}{2}\nu \frac{\partial^2}{\partial x_j^2}\left\langle u_i' u_i' \right\rangle}_{\text{Viscous Diffusion}} \underbrace{- \nu \left\langle \frac{\partial u_i'}{\partial x_j}\frac{\partial u_i'}{\partial x_j} \right\rangle}_{\text{Dissipation}}. \tag{12}$$

Equation 12 states that kinetic energy is affected by transport of velocity and pressure fluctuations and viscous stress along with dissipation and production of turbulence, which are the more relevant terms. The dissipation rate performs the exchange between the mean flow and turbulent fluctuations and the production rate performs the conversion of turbulent kinetic energy into internal energy (Tennekes *et al.*, 1972; Trofimova *et al.*, 2009).

Results for the TKE budget in the near-interface region for the stratified flow, normalized by ν/u_τ^4, compared with the single-phase flow are presented in Fig. 5, where different terms of the TKE budget are presented by different colors: the shear production rate is presented in black, the viscous difusion rate in blue, the turbulent transport rate in red and the viscous dissipation rate in green (for color reference please refer to the on-line version of the paper).

The behaviour of viscous difusion rate and turbulent transport rate did not change between single-phase and stratified flow, however, some minor changes are present in shear production rate. The near-interface peak is slightly lower than near-wall peak which suggest a certain amount of damping in the near-interface region against the near-wall region. This behaviour was extensively commented in literature (Fulgosi *et al.*, 2003)

As shown in de Azevedo *et al.* (2021), the viscous dissipation rate determination was a limitation of the present methodology, however, some differences are present in the results of single-phase flow and stratified flow. The near-interface values presented smaller dissipation rate than near-wall values owing to turbulence damping, as also commented by Fulgosi *et al.* (2003) in their work.

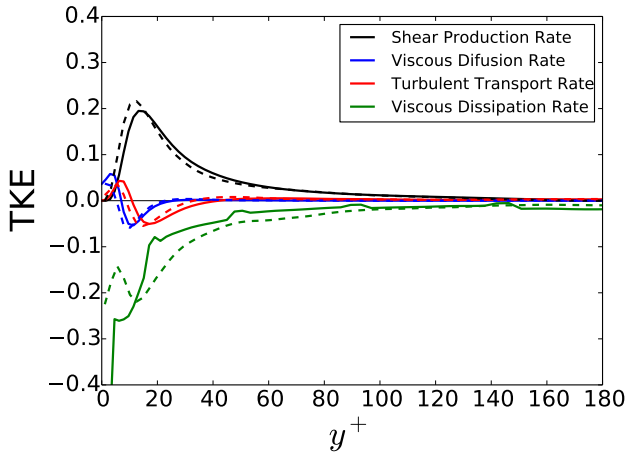

Figure 5: Turbulent kinetic energy budget: (-) denotes near-interface for the stratified flow values and (- -) denotes near-wall values for the single-phase flow.

3.4 Turbulent structures

Turbulent structures are identified through invariants of the velocity gradient tensor. There are different ways to characterize a turbulent structure, where decomposition of velocity gradient tensor in rate of strain S and rate of rotation Ω tensors, also known as Q criterion (Hunt *et al.*, 1988) is one of the most common present in literature, as defined in Eq. 13.

$$Q = \frac{1}{2}\left\langle \boldsymbol{\Omega}_{ij}\boldsymbol{\Omega}_{ij} - \boldsymbol{S}_{ij}\boldsymbol{S}_{ij} \right\rangle \tag{13}$$

Eq. 13 states that when $Q > 0$ the contribution of vorticity is greater than of the rate of strain in vortices areas, *i.e.*, the vortex core is represented by positive values of Q (Dupont and Brunet, 2009; Zhan *et al.*, 2019)

The Q criterion is one of the simplest ways to visualize turbulent structures and was used in the present work for flow visualization. Results for iso-volumes of constant Q are show in Fig. 6 for the near-interface and -wall regions of the stratified flow (Fig. 6a for near-interface region and Fig. 6b for the near-wall region). Coherent structures are noted in both regions, however, the predominancy of lines is evident in near-interface region (see the zoom view in Fig. 6a) against the near-wall region.

Even though is not possible to identify precisely the represented structures in the well-known family of coherent structures, one can note that the interface deformation captured by VOF, even being very small (see Fig. 7), induces some differences in flow structure when the near-interface region is compared to the near-wall region, which was also reflected in the turbulent statistics showed earlier in the present work.

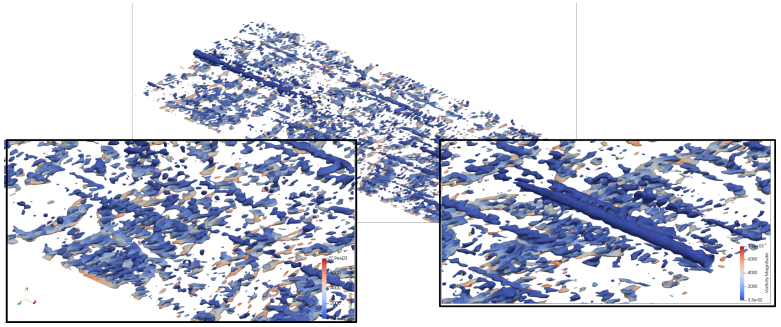

(a)

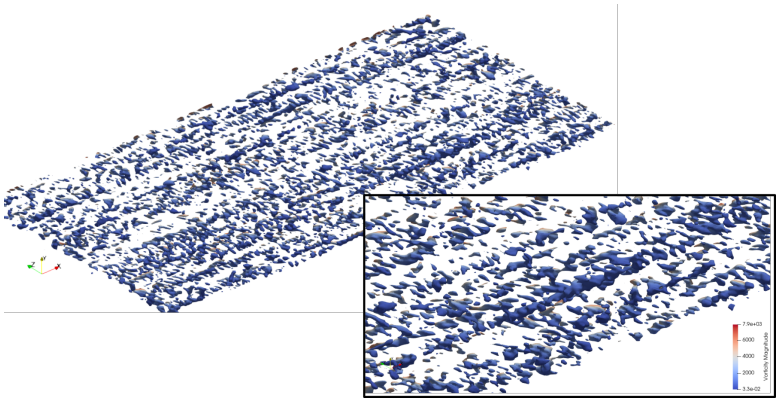

(b)

Figure 6: Q criterion application in the (a) near-interface region and (b) near-wall region of the stratified flow. The colour scale represent the vorticity magnitude.

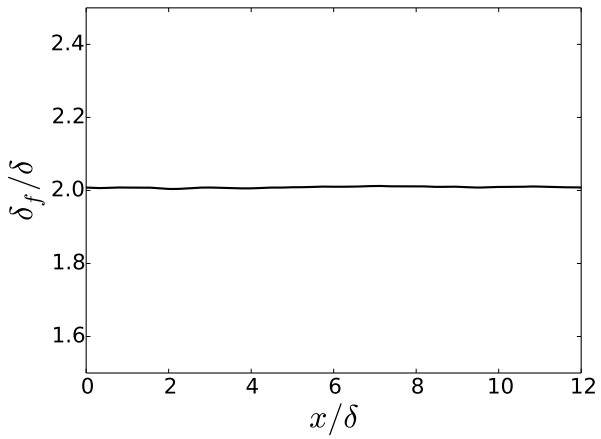

Figure 7: Interface deformation δ_f normalized by integral length scale δ. Very small waves in the capillary wave regime are present in the domain.

4. CONCLUSIONS

The present work developed DNS for wall-bounded stratified flow using Second-Order FVM to discretize the governing equations with solution in a VOF-framework. Results were validated by single-phase flow results obtained with the same methodology.

Near-interface turbulence statistics showed near-wall-like behaviour for velocity fluctuation and autocorrelation functions in the stream-wise direction. Small differences were noted in the TKE results for the shear production and viscous dissipation rates between near-wall and -interface simulations, which suggested the presence of a certain amount of turbulence damping in the near-interface region. The obtained results made also possible the visualization of coherent structures in the flow, even though it was not in the scope of the present work a complete analysis of turbulent structures in stratified flows.

The present model showed the viability of FVM and VOF application in multiphase flows with large scales deformable interfaces, which leaves open its application to another flow patterns.

5. ACKNOWLEDGEMENTS

The authors acknowledge the National Laboratory for Scientific Computing (LNCC/MCTI, Brazil) for providing HPC resources of the SDumont supercomputer, which have contributed to the research results reported within this paper.

6. REFERENCES

de Angelis, V., Lombardi, P. and Banerjee, S., 1997. "Direct numerical simulation of turbulent flow over a wavy wall". *Physics of Fluids (1994-present)*, Vol. 9, No. 8, pp. 2429–2442.

de Azevedo, V.W., Denner, F., Evrard, F. and Paladino, E.E., 2021. "Performance evaluation of standard second-order finite volume method for dns solution of turbulent channel flow". *Journal of the Brazilian Society of Mechanical Sciences and Engineering*, Vol. 43, No. 11, pp. 1–15.

Denner, F. and van Wachem, B.G., 2014. "Fully-coupled balanced-force vof framework for arbitrary meshes with least-squares curvature evaluation from volume fractions". *Numerical Heat Transfer, Part B: Fundamentals*, Vol. 65, No. 3, pp. 218–255.

Denner, F. and van Wachem, B.G., 2015. "Numerical time-step restrictions as a result of capillary waves". *Journal of Computational Physics*, Vol. 285, pp. 24–40.

Dupont, S. and Brunet, Y., 2009. "Coherent structures in canopy edge flow: a large-eddy simulation study". *Journal of Fluid Mechanics*, Vol. 630, pp. 93–128.

Eggels, J., Westerweel, J., Nieuwstadt, F. and Adrian, R., 1993. "Direct numerical simulation of turbulent pipe flow". In *Advances in Turbulence IV*, Springer, pp. 319–324.

Egorov, Y., Boucker, M., Martin, A., Pigny, S., Scheuerer, M. and Willemsen, S., 2004. "Validation of cfd codes with pts-relevant test cases". *5th Euratom Framework Programme ECORA project*, Vol. 2004, pp. 91–116.

Fan, W. and Anglart, H., 2019. "Progress in phenomenological modeling of turbulence damping around a two-phase interface". *Fluids*, Vol. 4, No. 3, p. 136.

Frederix, E., Mathur, A., Dovizio, D., Geurts, B. and Komen, E., 2018. "Reynolds-averaged modeling of turbulence damping near a large-scale interface in two-phase flow". *Nuclear Engineering and Design*, Vol. 333, pp. 122–130.

Fulgosi, M., Lakehal, D., Banerjee, S. and de Angelis, V., 2003. "Direct numerical simulation of turbulence in a sheared air–water flow with a deformable interface". *Journal of fluid mechanics*, Vol. 482, pp. 319–345.

Hunt, J.C., Wray, A.A. and Moin, P., 1988. "Eddies, streams, and convergence zones in turbulent flows". *Studying turbulence using numerical simulation databases, 2. Proceedings of the 1988 summer program*.

Kim, J., Moin, P. and Moser, R., 1987. "Turbulence statistics in fully developed channel flow at low reynolds number". *Journal of fluid mechanics*, Vol. 177, pp. 133–166.

Lakehal, D., Reboux, S. and Liovic, P., 2005. "Sub-grid scale modelling for the les of interfacial gas-liquid flows". *Houille Blanche*, Vol. 6, No. 05, p. 1.

Liovic, P. and Lakehal, D., 2007. "Multi-physics treatment in the vicinity of arbitrarily deformable gas–liquid interfaces". *Journal of Computational Physics*, Vol. 222, No. 2, pp. 504–535.

Lombardi, P., de Angelis, V. and Banerjee, S., 1996. "Direct numerical simulation of near-interface turbulence in coupled gas-liquid flow". *Physics of Fluids (1994-present)*, Vol. 8, No. 6, pp. 1643–1665.

Pope, S.B., 2001. "Turbulent flows".

Silveira Neto, A.d., 2020. *Escoamentos Turbulentos: Análise Física e Modelagem Teórica (in portuguese)*. Composer.

Tekavčič, M., Meller, R. and Schlegel, F., 2021. "Validation of a morphology adaptive multi-field two-fluid model considering counter-current stratified flow with interfacial turbulence damping". *Nuclear Engineering and Design*, Vol. 379, p. 111223.

Tennekes, H., Lumley, J.L., Lumley, J. *et al.*, 1972. *A first course in turbulence*. MIT press.

Trofimova, A.V., Tejada-Martínez, A.E., Jansen, K.E. and Lahey Jr, R.T., 2009. "Direct numerical simulation of turbulent channel flows using a stabilized finite element method". *Computers & Fluids*, Vol. 38, No. 4, pp. 924–938.

Ubbink, O. and Issa, R., 1999. "A method for capturing sharp fluid interfaces on arbitrary meshes". *Journal of Computational Physics*, Vol. 153, No. 1, pp. 26–50.

Zhan, J.m., Li, Y.t., Wai, W.h.O. and Hu, W.q., 2019. "Comparison between the q criterion and rortex in the application of an in-stream structure". *Physics of Fluids*, Vol. 31, No. 12, p. 121701.

Zonta, F., Onorato, M. and Soldati, A., 2016. "Decay of gravity-capillary waves in air/water sheared turbulence". *International Journal of Heat and Fluid Flow*, Vol. 61, pp. 137–144.

7. RESPONSIBILITY NOTICE

The authors are the only responsible for the printed material included in this paper.